Supplement: Saharan warm air intrusions in the Western Mediterranean: identification, impacts on temperature extremes and large-scale mechanisms

Pep Cos[1,2], Matias Olmo[1], Diego Campos[1,2], Raül Marcos-Matamoros[2], Lluis Palma[1,2], Ángel G. Muñoz[1], and Francisco J. Doblas-Reyes[1,3]

[1]Earth Sciences Department, Barcelona Supercomputing Center (BSC), Barcelona, Spain
[2]Department of Applied Physics, University of Barcelona, Barcelona, Spain
[3]Institució Catalana de Recerca i Estudis Avançats (ICREA), Barcelona, Spain

Correspondence: Pep Cos (josep.cos@bsc.es)

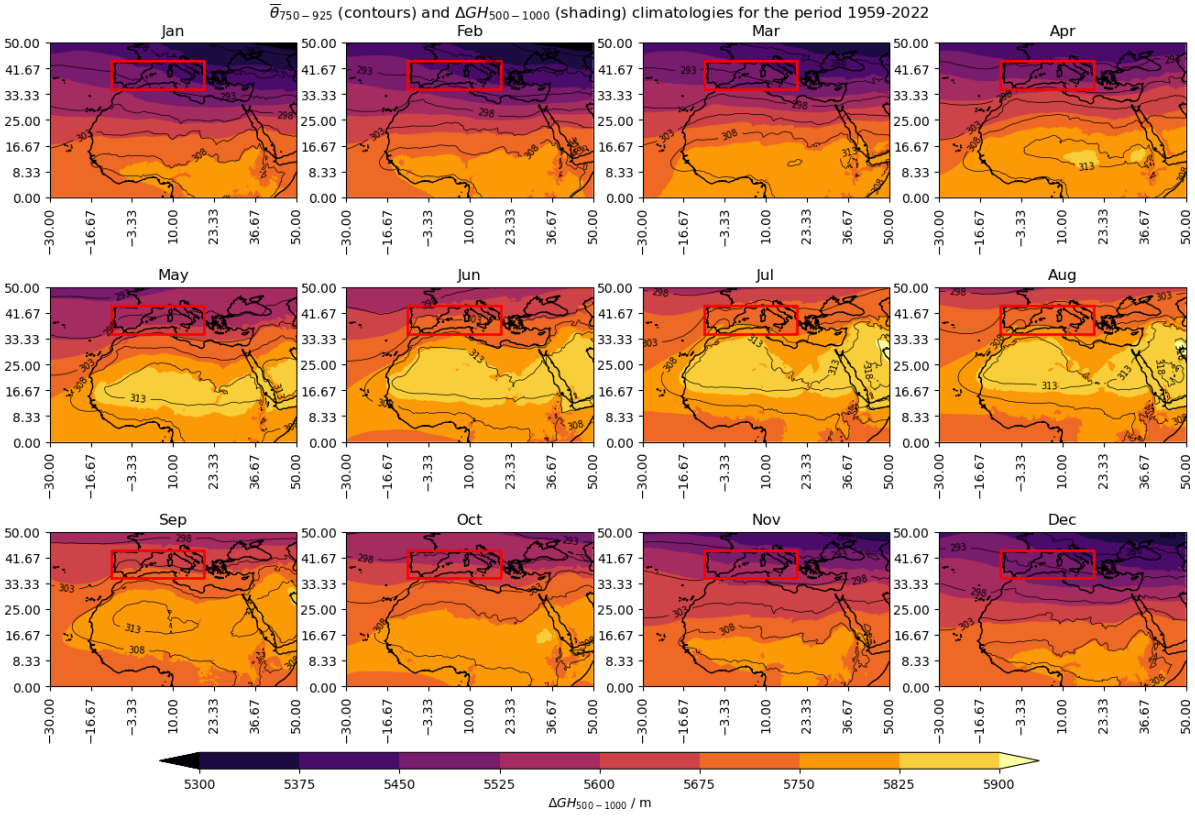

Figure S1. $\Delta GH_{500-1000}$ and $\overline{\theta}_{750-925}$ monthly climatologies during the period 1959-2022. The red box is the area of the Sahara desert used as reference to compute the thresholds for the intrusion identification metrics.

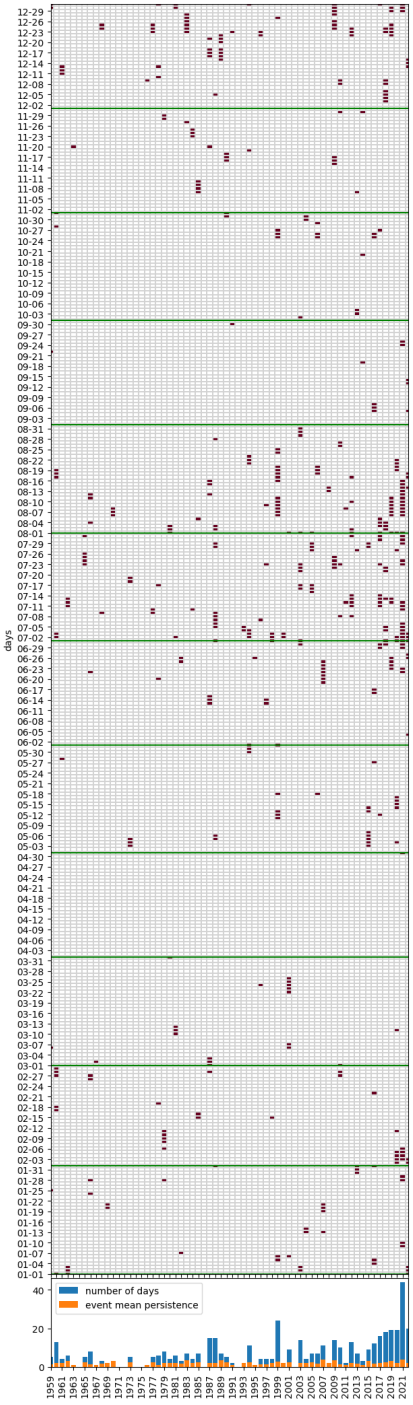

Figure S2. Historical catalogue of intrusion days in the period 1959-2022 (x-axis) and from the 1st of January to the 31st of December (y-axis). The days identified as intrusions are coloured in dark red. Green lines indicate the transition between months. The yearly number of intrusion days (blue) and the mean persistence (orange) are shown at the bottom.

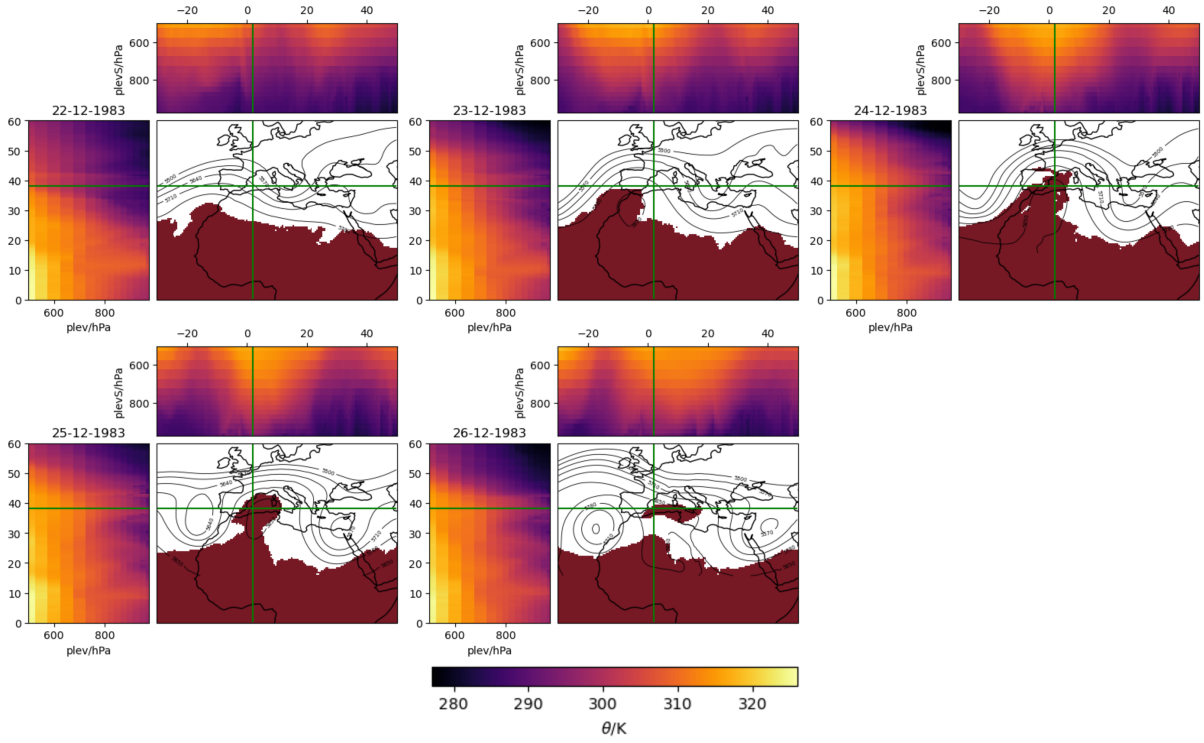

Figure S3. Same as Figure 3 but for the intrusion event observed in the period 23/12/1983 to 26/12/1983. The event is preceded by an intense trough developed in the North Atlantic that forces a subtropical ridge over the Western Mediterranean and pushes a Saharan air mass (same as subtropical air mass in this case, as red is present in all the longitudinal band below 25º N) towards the Iberian Peninsula. The event is maintained by an omega block formed by a high pressure system over Europe, a low west of Iberia and a low over the Eastern Mediterranean. The vertical distribution of the potential temperature is also distinct and more homogeneous in the regions where the intrusion is present, but to a lesser extent than the summer event shown in Figure 3. At the end of the event, although the blocking persists, the air mass starts losing its properties and some detached subtropical-like masses can be seen north of Africa.

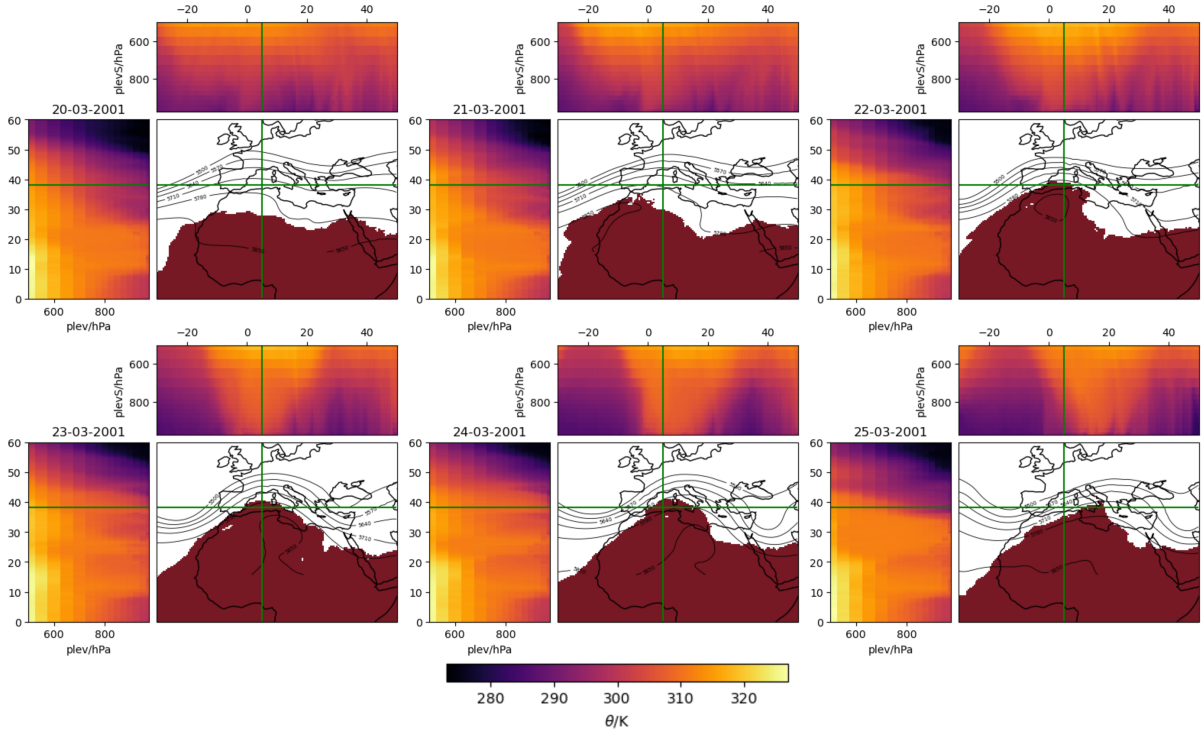

Figure S4. Same as Figure 3 but for the intrusion observed in the period 20/03/2001 to 25/03/2001. The event is preceded by a slight trough developed in the North Atlantic that forces a subtropical ridge over the Western Mediterranean and pushes a Saharan air mass towards the central WMed. In this case the intrusion propagates from West to East and from South to North and back South to Africa. The $\overline{\theta}_{750-925}$ vertical cuts show how the air mass is very warm and vertically homogeneous.

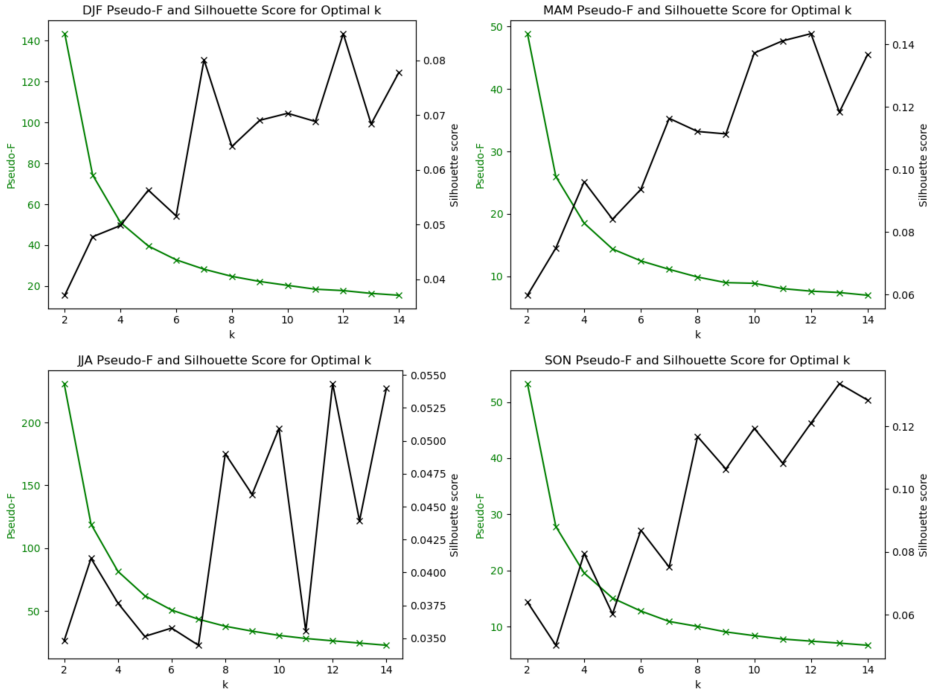

Figure S5. Silhouette (black) and Pseudo-F (green) scores as a function of the number of clusters for the DJF, MAM, JJA and SON seasons.

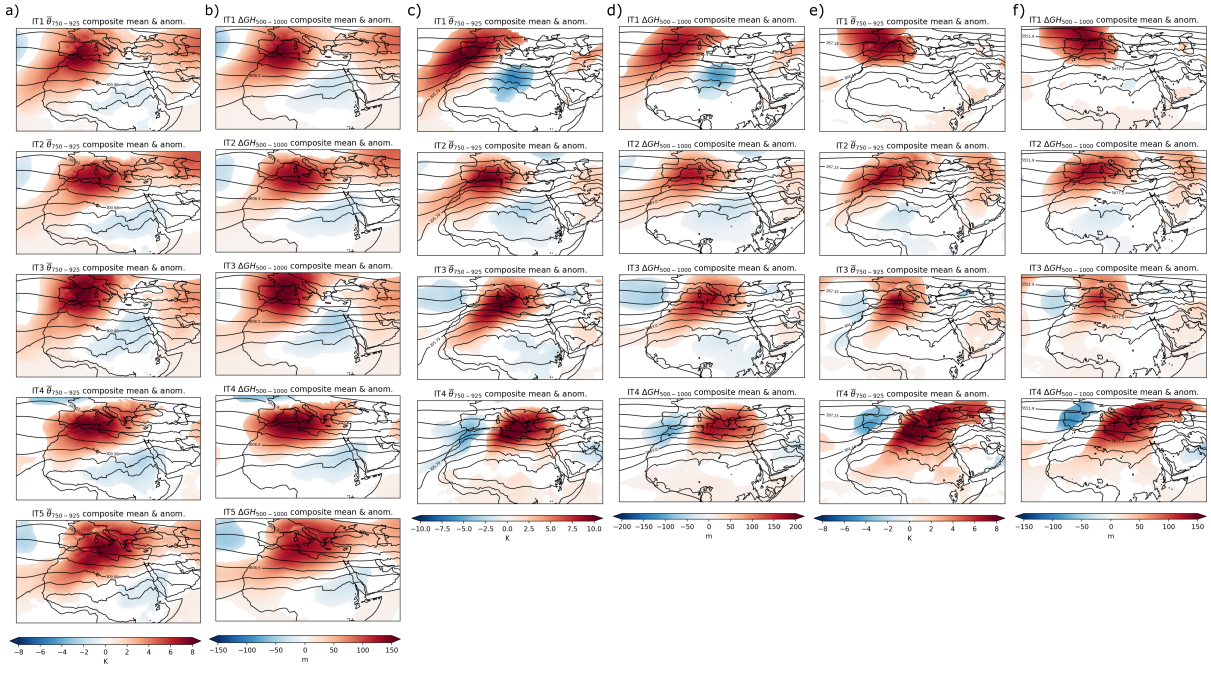

Figure S6. Same as Figure 5 but for DJF (a,b), MAM (c,d) and SON (e,f)

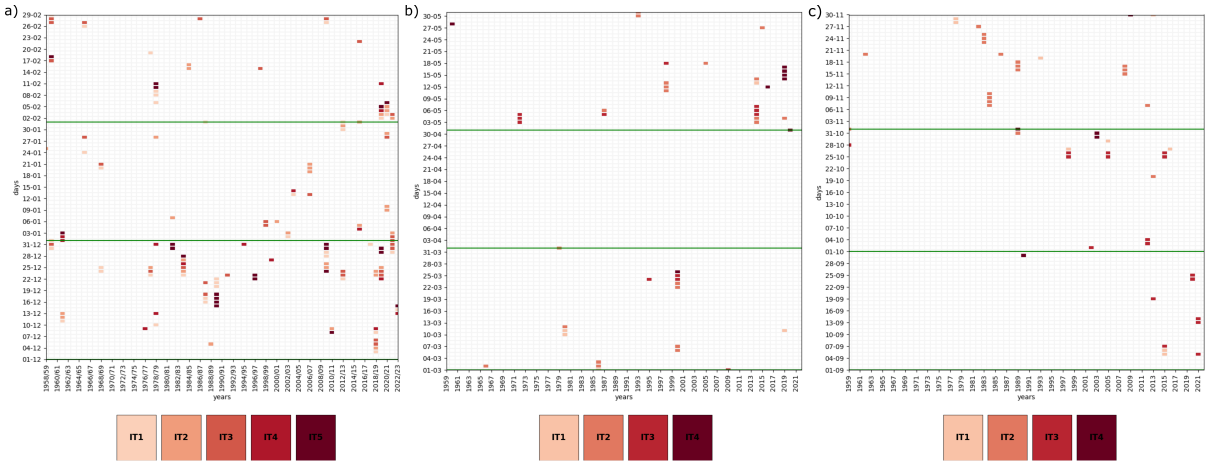

Figure S7. Same as Figure 5 but for a) DJF, b) MAM and d) SON.

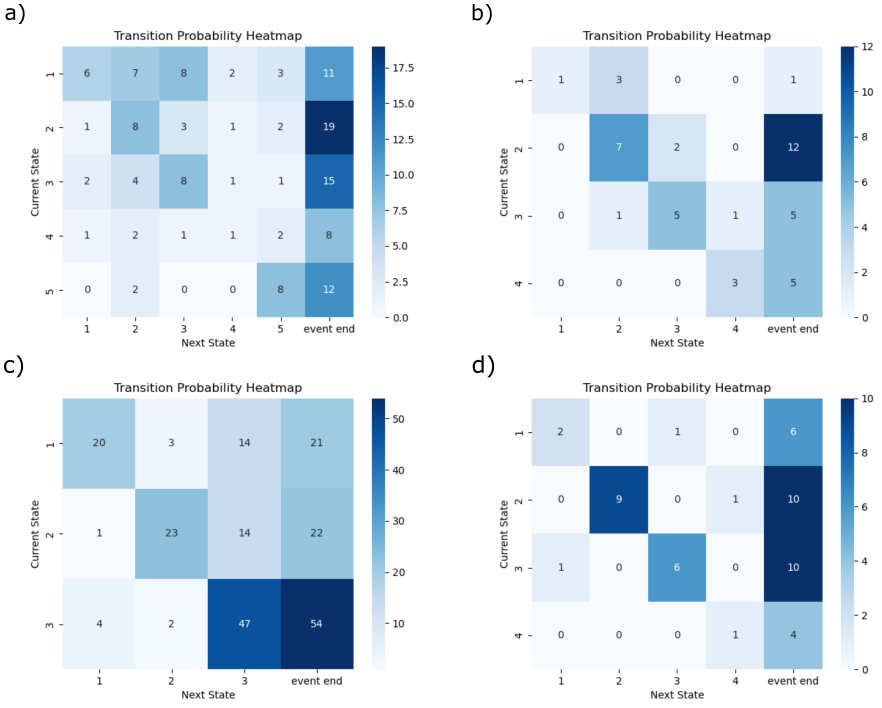

Figure S8. Transition probability heatmap showing the number of times that an intrusion day transitioned from one IT (current state) to another IT (next state) for a) DJF, b) MAM c) JJA d) SON. The next state axis has an extra column showing the amount of days that an intrusion event ended in a particular IT.

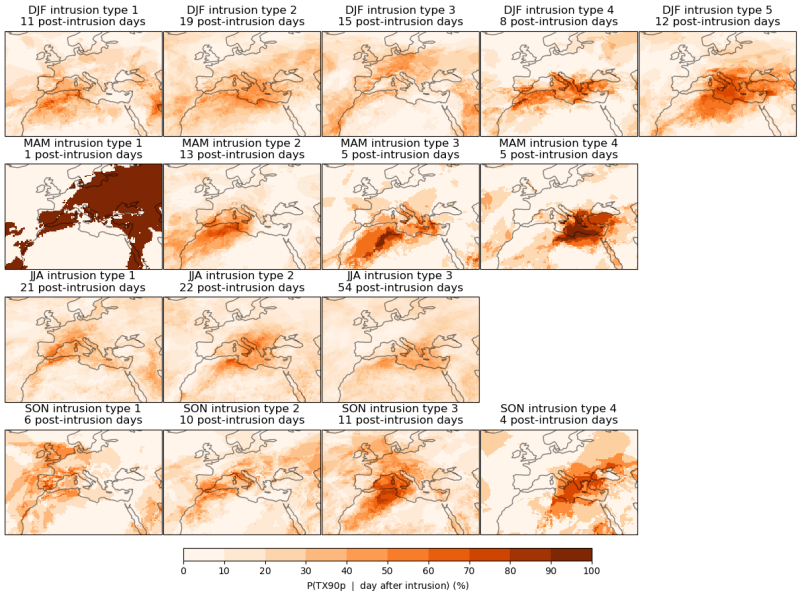

Figure S9. Impact of the days after an intrusion event on extreme temperatures in the EM region for the different seasons (rows) and ITs (columns). The impact is measured as the percentage of days after an intrusion event that coincide with an extreme temperature day (TX90p). The amount of days after an intrusion event for each season and IT is specified in the title of each panel (Note that MAM IT1 has only one day and hence the values can only be 100% or 0%).

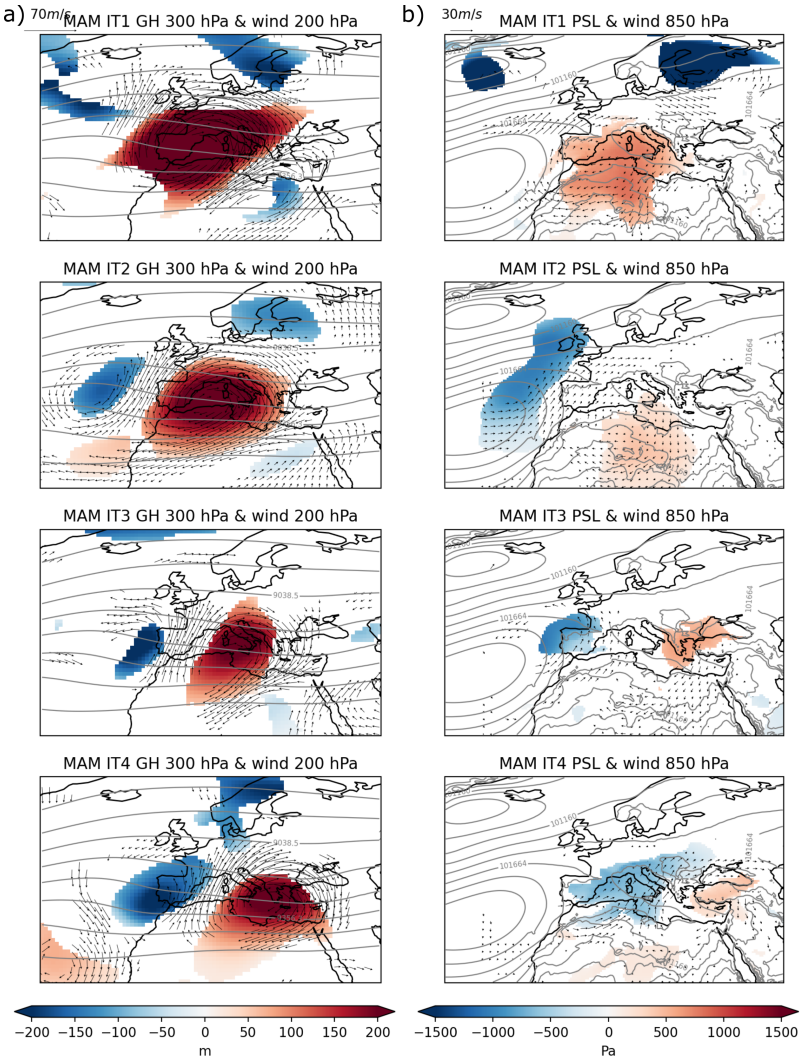

Figure S10. Same as Figure 9 but for the MAM ITs.

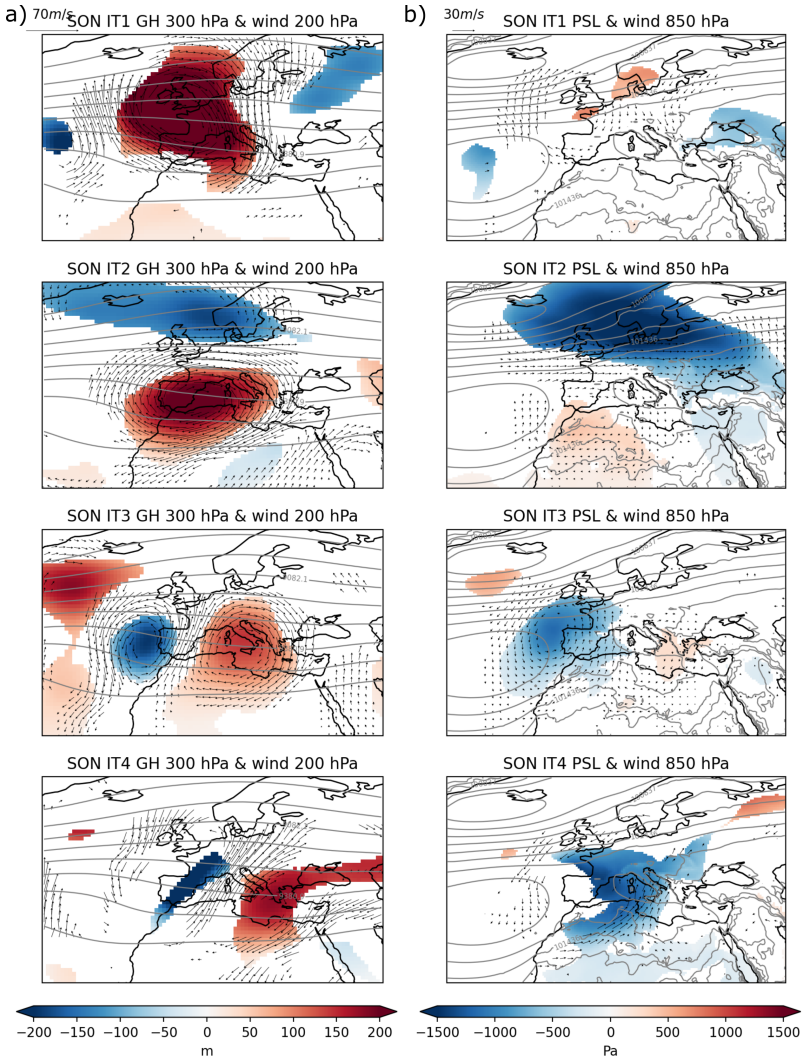

Figure S11. Same as Figure 9 but for the SON ITs.

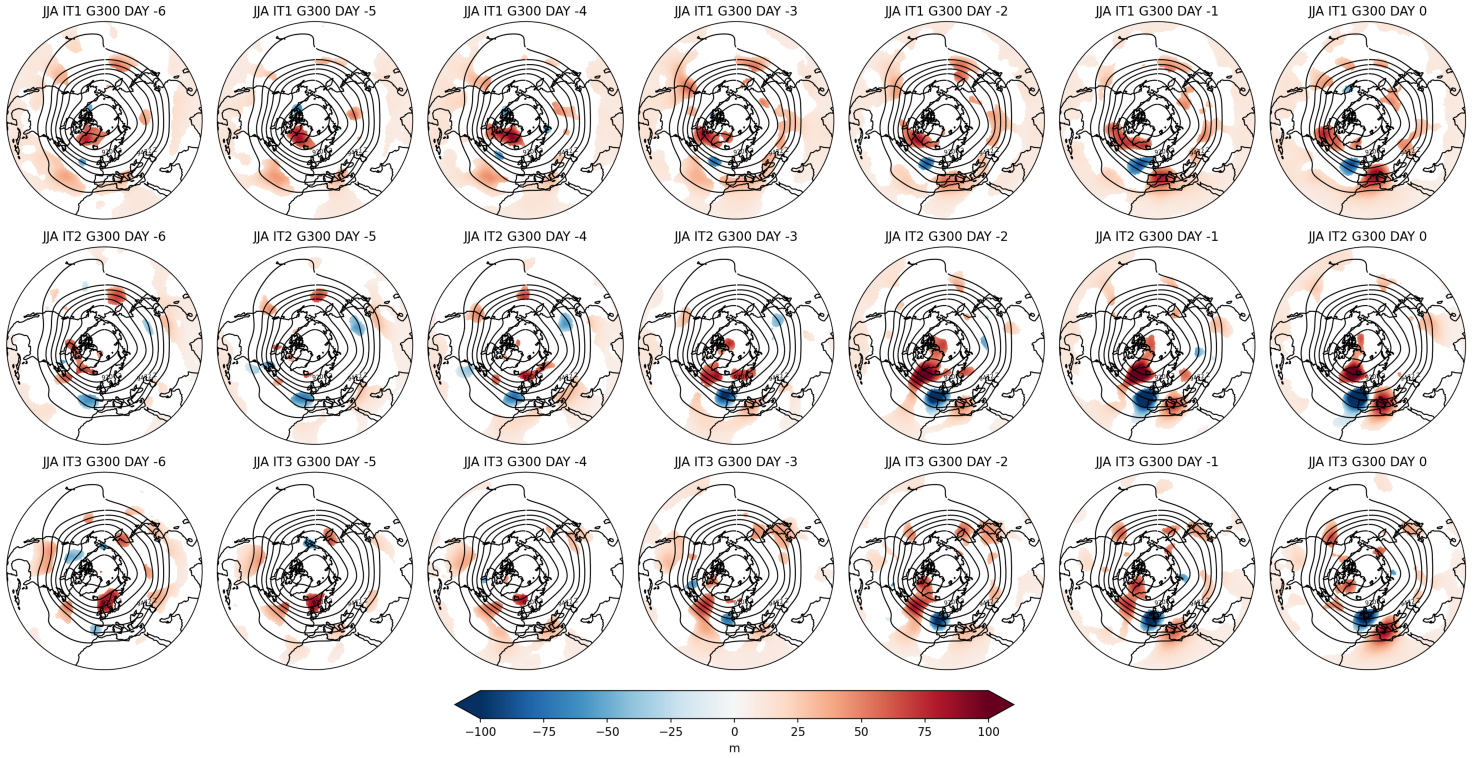

Figure S12. JJA composites of the first day (right) and the 6 days (right to left) prior to the intrusion events (columns) for geopotential height (shading) at 300 hPa for the three ITs (rows). Anomalies computed with respect to the non-intrusion climatologies of 7-day moving windows centred on each calendar day between 1959-2022. Contours show the climatological 300 hPa geopotential height. No values are shown where the anomaly is not significantly different to 0 with a t-Student test and 95% confidence level.

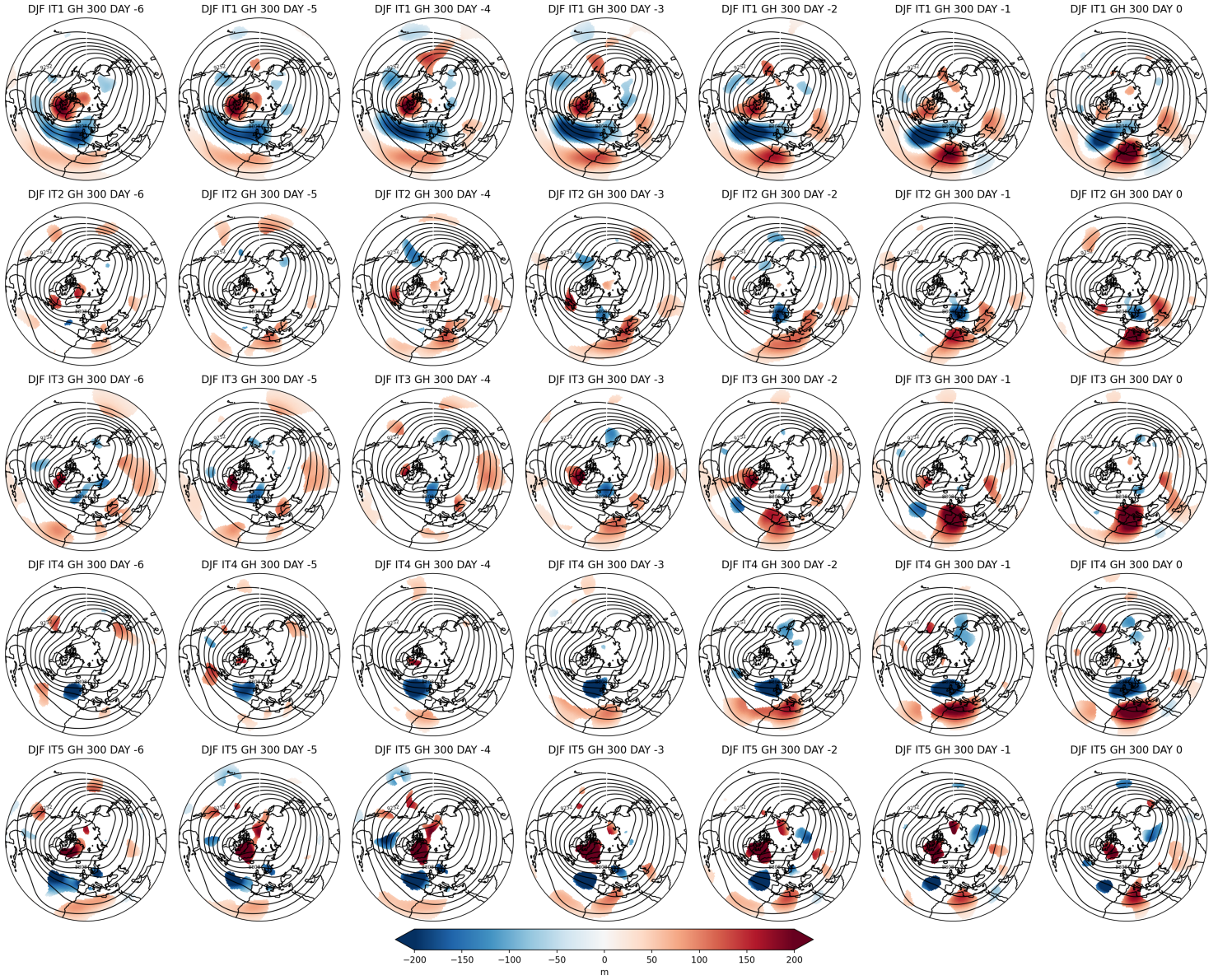

Figure S13. Same as S12 but for DJF